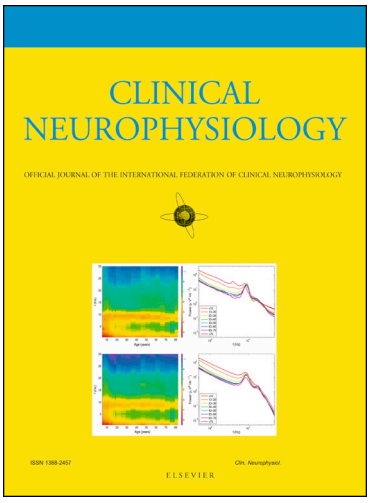

Temporal-spatial characteristics of phase-amplitude coupling in electrocorticogram for human temporal lobe epilepsy

Ruihua Zhang, Ye Ren, Chunyan Liu, Na Xu, Xiaoli Li, Fengyu Cong, Tapani Ristaniemi, YuPing Wang

PII: S1388-2457(17)30216-X
DOI: http://dx.doi.org/10.1016/j.clinph.2017.05.020
Reference: CLINPH 2008166

To appear in: *Clinical Neurophysiology*

Received Date: 15 February 2017
Revised Date: 27 April 2017
Accepted Date: 31 May 2017

Please cite this article as: Zhang, R., Ren, Y., Liu, C., Xu, N., Li, X., Cong, F., Ristaniemi, T., Wang, Y., Temporal-spatial characteristics of phase-amplitude coupling in electrocorticogram for human temporal lobe epilepsy, *Clinical Neurophysiology* (2017), doi: http://dx.doi.org/10.1016/j.clinph.2017.05.020

Temporal-spatial characteristics of phase-amplitude coupling in electrocorticogram for human temporal lobe epilepsy

Authors: Ruihua Zhang[a,b,1], Ye Ren[b,c,1], Chunyan Liu[a], Na Xu[b], Xiaoli Li[d], Fengyu Cong[c,e], Tapani Ristaniemi[c], YuPing Wang[a,f,g*]

Affiliations:

[a] Department of Neurology, Xuanwu Hospital, Capital Medical University, Beijing, 100053, China

[b] Department of Geriatric Medicine, Beijing Luhe Hospital, Capital Medical University, Beijing, 101149, China

[c] Department of Mathematical Information Technology, Faculty of Information Technology, University of Jyväskylä, Jyväskylä, 40014, Finland

[d] State Key Laboratory of Cognitive Neuroscience and Learning & IDG/McGovern Institute for Brain

Research, Beijing Normal University, Beijing, 100875, China

[e] Department of Biomedical Engineering, Faculty of Electronic Information and Electrical Engineering, Dalian University of Technology, Dalian, 116024, China

[f] Beijing Key Laboratory of Neuromodulation, Beijing 100053, China

[g] Center of Epilepsy, Beijing Institute for Brain Disorders, Beijing 100053, China

* Corresponding author: Yuping Wang

Address: No.45, Changchun Street, Xicheng District, Beijing, 100053, China

Email: wangyupingcn@163.com

Telephone: +86 15910380817

Fax: +86 (0)10 69543901-1051

[1] These authors contributed equally to this work.

Hightlights

- PAC could be a good tool for lateralization and localization for the epileptic focus.
- "Fall-max" pattern was found to be a reliable biomarker in middle seizure period.
- Strong PAC was appeared mainly between δ、θ、α oscillations and γ、ripple oscillations.

Abstract

Objective: Neural activity of the epileptic human brain contains the low-frequency and high-frequency oscillations in different frequency bands, some of which have been used as the reliable biomarkers of the epileptogenic brain areas. However, the relationship between the low-frequency and high-frequency oscillations at different cortical areas during the period from pre-seizure to post-seizure has not been completely clarified.

Methods: We recorded the electrocorticogram data from the temporal lobe and hippocampus of seven patients with temporal lobe epilepsy. The modulation index based on the Kullback-Leibler distance and the phase-amplitude coupling co-modulogram were adopted to quantify the coupling strength between the phase of low-frequency oscillations (0.2-10 Hz) and the amplitude of high-frequency oscillations (11-400 Hz) at different seizure epochs. The time-varying phase-amplitude modulogram was used to analyze the phase-amplitude coupling pattern during the whole period from pre-seizure to post-seizure at both left and right temporal lobe and hippocampus. Channels with strong modulation index were compared with the seizure onset channels identified by the neurosurgeons and the resection channels in the clinical surgery.

Results: The phase-amplitude coupling strength (modulation index) increased significantly at mid-seizure epoch and decrease significantly at seizure-termination and post-seizure epochs (p<0.001). The strong phase-amplitude modulating low-frequency and high-frequency oscillations at mid-seizure epoch were mainly δ、θ、α oscillations and γ、ripple oscillations, respectively. The phase-amplitude modulation and strength varied among channels and was asymmetrical on the left

and right temporal cortex and hippocampus. “Fall-max” phase-amplitude modulation pattern, i.e. the high-frequency amplitudes were largest at the low-frequency phase range [-π, 0] which corresponded to the falling edges of low-frequency oscillations, appeared in the middle period of the seizures at epileptic focus channels. Channels with strong modulation index appeared on the corresponding left or right temporal cortex of surgical resection and overlapped with the clinical resection zones in all patients.

Conclusions: The “fall-max” pattern between the phase of low-frequency oscillation and amplitude of high-frequency oscillation appeared in the middle period of the seizures is a reliable biomarker in epileptogenic cortical areas. The modulation index can be used as a good tool for lateralization and localization for the epileptic focus for patients with epilepsy.

Significance: Phase-amplitude coupling can provide meaningful reference for accurate resection of epileptogenic focus and also provide insight to the underlying neural dynamics of the epileptic seizure for patients with temporal lobe epilepsy.

Keywords: ECoG; temporal lobe epilepsy; cross-frequency coupling; modulation index; fall-max pattern

1. Introduction

Abnormal discharge of neurons in the epileptic human brain causes the specificity of the neural oscillations of the cerebral cortex. The low-frequency and high-frequency neural oscillations of some frequency bands have been known as the essential biomarkers of the epileptogenicity and epileptic seizure-onset zones. The dynamic process of very low frequency oscillations (LFOs) in the intracranial electroencephalographic recordings has been found to occur during the preictal state in the refractory epilepsy patients (Ren et al. , 2011). The ictal infraslow activity and ictal high frequency oscillations (HFOs) were both represented the core of tissue generating seizures in epileptic patients (Imamura et al. , 2011, Kanazawa et al. , 2015). Also, Crépon et al. used the semi-automatic detection procedure of wavelet decomposition to confirm the generation of interictal high-frequency oscillations over 200 Hz in medial and polar temporal lobes, which was regarded as a reliable marker of the seizure onset zone (Crépon et al. , 2010). Resection of the cortical areas generating fast ripples (>200 Hz) and ripples on a flat background activity has also been found to show a significant correlation with seizure-free outcome (Kerber et al. , 2014). Besides, temporal changes of ripples (100-250 Hz) and fast ripples (250-500 Hz) during different seizure periods have been found to vary greatly between individual epileptic patients (Pearce et al. , 2013). These LFOs and HFOs that occur in patients with epilepsy have been considered potential biomarkers of epileptogenesis. However, they offered limited insight into the feature of neural oscillations during the epileptic seizures because the complex neural activities in the epileptic cerebral cortex are constituted by simultaneous neural oscillations in different frequency bands.

The interactions between neural oscillations in different frequency bands, which are termed as

cross-frequency coupling (CFC), play an important role in investigating the mechanisms of the communication and connectivity in neural networks. Phase-amplitude coupling (PAC), one form of CFC, in which the phase of LFO modulates the amplitude of HFO, has become a rising concern in recent studies. Alvarado-Rojas et al. used the cross-frequency PAC in ECoG of patients with partial epilepsy to predict the seizures (Alvarado-Rojas et al. , 2011). CFC between the amplitude of pathological high-frequency oscillations and the phase of theta and alpha rhythms was found to be significantly elevated in seizure-onset zone compared to non-epileptic regions in patients with partial epilepsy (Ibrahim et al. , 2014). Moreover, Guirgis et al. adopted the measures of modulation index and eigenvalue decomposition to confirmed that delta-modulated high-frequency oscillations could provide more accurate localization of epileptogenic zone in extratemproal lobe epileptic patients (Guirgis et al. , 2015a). Recently, modulation index was also used to determine the predictive accuracy of seizure onset sites and eloquent areas in children with focal epilepsy, which suggested the epileptogenic HFOs might be coupled with slow-wave 3-4 Hz more preferentially than slow-wave 0.5-1 Hz (Nonoda et al. , 2016). Also, PAC was estimated by the synchronization index for ECoG from patients with refractory temporal lobe epilepsy and accurately distinguished the ictal state from interictal state with strong coupling between the phase of beta oscillation and the amplitude of high gama oscillation (Edakawa et al. , 2016).

Previous studies concentrated more on the coupling strength, coupling frequency bands or coupling areas of the brain between the phase of LFO and the amplitude of HFO. However, the coupling patterns of phase-amplitude interaction in different brain areas during the non-seizure and seizure periods still remain unclear. Therefore, the aims of this study are to investigate whether the PAC

differs in different seizure periods and in what forms the low-frequency phase and high-frequency amplitude may couple. Also, we aim to estimate whether the PAC differs in left and right temporal cortex and hippocampi of patients with temporal lobe epilepsy.

To address and better understand these issues, we collected the eletrocorticogram (ECoG) data from the left and right temporal cortex and hippocampi in seven patients with temporal lobe epilepsy. We adopted the modulation index based on the Kullback-Leibler distance (Tort et al. , 2010), PAC co-modulogram and time-varying phase-amplitude modulogram (Mukamel et al. , 2011) to explore the temporal-spatial characterization of the PAC strength and patterns during the period from pre-seizure to post-seizure at both sides of the cortex (see Materials and methods for details).

2. Materials and methods

2.1 Data recordings and preprocessing

We obtained the ECoG recordings from subdural strip electrodes implanted in seven patients. Six patients were presented with suspected bilateral temporal lobe epilepsy and the other was right temporal lobe epilepsy. All patients provided written informed consent, approved by the ethical committee of Xuanwu Hospital (Patient A, B, C and D) and Luhe Hospital (Patient E, F and G). All seven patients are pathologically focal cortical dysplasia (FCD). The clinical characteristics of each patient are summarized in Table 1. The cortical electrode strip (2.5mm diameter platinum electrodes positioned 10mm apart center-to center) and depth electrode strip (1.2mm diameter platinum electrodes positioned 10mm apart center-to center) was implanted on the temporal lobes and hippocampi of each patient respectively. All electrode strips are placed symmetrically on the left and right cerebral cortex except patient E. The strips of patient E are placed only in the right cerebral cortex. The spatial distribution of preoperative intracranial electrode strips of patient A is shown in Fig. 1A. The top panel shows the left and right views of cerebral cortex, the bottom panel shows the top and upward views of cerebral cortex. We arranged all the electrode strips in the plane (Fig. 1B), which could be observed easily.

ECoG signals were continuously recorded day and night for preoperative assessment of all patients, using a video-EEG monitoring system (PN-NET, Beijing Yunshen Technology, China). An electrode located far away from the epileptic focus was used as the reference electrode. The sampling frequency of the ECoG data is 2048 Hz. The ECoG data were exported as European Data Format Plus (EDF+) files and imported into EEGLAB for changing the file format to MAT. We recorded the

ECoG data of 16 seizures across 7 patients in total and selected 12 seizures for analysis, which included the complete spontaneous epileptic seizures from each patient. The data of other four seizures were not used for analysis because of the incomplete data recording, which did not contain the data in pre-seizure or post seizure period. All ECoG data segments were selected from about 1 minute before seizure onset time to about 1 minute after seizure termination time. The ECoG data segments were downsampled to 1024 Hz firstly and filtered by a 0.2 Hz high-pass filter for removing baseline interference. Power frequency noise (50Hz) and harmonic noises were then removed by the notch filter. We also removed the large amplitude artifacts in the ECoG data and rejected the bad channels by visual inspection from each patient. Fig. 2A shows the preprocessed ECoG data of channel 38 from patient A. Both the seizure onset time (t_{SO}) and the seizure termination time (t_{ST}) were determined by neurologists clinically and labeled on the time coordinate. The seizure onset channels were also clinically defined as the electrodes with earliest ictal activity, named focal fast waves.

[Insert Fig. 1]

[Insert Table 1]

[Insert Fig. 2]

2.2 Phase-amplitude coupling analysis

Modulation index (MI) based on the Kullback-Leibler distance (Tort et al. , 2010) was adopted to quantify the strength of PAC. Time-varying phase-amplitude modulogram (Mukamel et al. , 2011) was used to characterize the PAC pattern between two specific frequency bands during the period from pre-seizure to post-seizure.

The computing process for PAC was described in Fig. 3, including the following steps:

(i) Filter the ECoG data $X(t)$ by a bandpass filter (*eegfilt.m* in EEGLAB toolbox) to construct a

narrow band low-frequency signal $X_L(t)$ and a high-frequency signal $X_H(t)$.

(ii) Extract the instantaneous phase $\varphi_L(t)$ and instantaneous amplitude $A_H(t)$ from $X_L(t)$ and $X_H(t)$ respectively by using the Hilbert transform.

(iii) Segment $\varphi_L(t)$ and $A_H(t)$ into 10-second epochs with an overlap of 90%. The phase and amplitude in each epoch k is denoted as $\varphi_{L_k}(t)$ and $A_{H_k}(t)$ $(k = 1,2,\cdots,K)$. Divide the phase range [-π,+π] into eighteen equally intervals (The length of each interval is π/9, N=18).

(iv) In each epoch k, assign all instantaneous phases of $\varphi_{L_k}(t)$ to one of the eighteen phase bins $j, j = 1,2,\cdots,N$. The instantaneous phase and their corresponding instantaneous amplitude are denoted as $\varphi_{L_{k,j}}(t)$ and $A_{H_{k,j}}(t)$, respectively. The mean amplitude at each phase bin j is denoted as $\langle A_{H_k}\rangle(j)$. Then we normalize the mean amplitudes over 18 phase bins $M_k(j) = \frac{\langle A_{H_k}\rangle(j)}{\sum_{j=1}^{N}\langle A_{H_k}\rangle(j)}$ to obtain the time-varying phase-amplitude modulogram.

(v) The modulation index is defined by dividing the KL distance of the modulogram distribution $M_k(j)$ from the uniform distribution $U(j)$ by $log(N)$.The MI is denoted as $MI = \frac{D_{KL}(M_k,U)}{log(N)}$, where the $D_{KL}(M_k,U) = \sum_{j=1}^{N} M_k(j) log\left[\frac{M_k(j)}{U(j)}\right]$.

(vi) Considering $U(j) = 1/N, j = 1,2,\cdots,N$, the MI can be denoted as $MI = \frac{\sum_{j=1}^{N} M_k(j) log M_k(j)}{log(N)} + 1$, which quantify the strength of PAC between LFOs and HFOs. The MI ranges from 0 to 1, where the MI value of 0 represents lack of PAC and the MI of 1 reflects strong PAC.

The narrow band low-frequency and high-frequency ECoG data were filtered at 0.2-10 Hz with the step of 0.1Hz and 11-400 Hz with the step of 1Hz, respectively. MI was computed between the narrow band low-frequency and high-frequency data in 10-second windows with an overlap of 90 %.

[Insert Fig. 3]

2.3 Statistical analysis

We assessed the statistical significance of *MI* by permutation test (Mukamel et al. , 2014). 200 random time shifts were generated from a uniform distribution on the interval [-5 s, 5 s]. We computed the permuted modulation index MI_{perm} using the original and the shifted amplitude. Then, *MI* was judged significant if it was larger than 95% of the 200 permuted values MI_{perm}. Matlab Statistics Toolbox was also applied for statistics. In order to assess the changes of PAC strength during the period from pre-seizure to post-seizure, we compared the *MI* values between specific LFOs and HFOs in five seizure epochs (pre-seizure, seizure onset, mid-seizure, seizure termination and post-seizure epoch) of each patient. We used the Kruskal-Wallis test (*kruskalwallis.m*) and Multiple comparison test (*multcompare.m*) to determine the significant difference of *MI* among different seizure epochs. The *MI* values were presented using the box plot. Also, *MI* values between seizure-specific LFOs and HFOs at mid-seizure epoch of all electrode channels of each patients were compared using the Kruskal-Wallis test (*kruskalwallis.m*) and Multiple comparison test (*multcompare.m*) to determine the significant difference of PAC strength cross all channels. $p<0.01$ was considered significant difference and marked with the notation *.

3. Results

3.1 Time varying phase-amplitude modulation during temporal seizure.

In order to quantify the strength of PAC of ECoG signals during seizure period for all patients, we computed the *MI* value along the whole period of all channels for each patient. To investigate the specificity of PAC in different time periods of temporal seizure, a 10-second pre-seizure, seizure onset, mid-seizure, seizure termination and post-seizure epoch were selected from all channels for each patient. Five seizure epochs in Patient A were shown with the gray rectangles marked on one channel ECoG signal in Fig. 2A. The seizure onset epoch was selected from t_{SO} to 10 seconds afterward and the seizure termination epoch was selected from t_{ST} to 10 seconds forward. The mid-seizure epoch was chosen 5 seconds before and after the middle time point of seizure period (from t_{SO} to t_{ST}). The pre-seizure and post-seizure epoch was selected approximately 30 seconds before and after the seizure onset and seizure termination epoch, respectively.

Then, we computed the *MI* between each low-frequency (0.2-10 Hz with the step of 0.1 Hz) phase and high-frequency (11-400 Hz with the step of 1 Hz) amplitude at five selected epochs from all channels of each patient, which constructed the PAC co-modulogram. The co-modulogram at each epoch from channel 38 (at right temporal base) of Patient A (Seizure 2) was shown in Fig. 2B. The frequency for amplitude was set at 11-200 Hz in the figure which made the *MI* values displayed enlarged. It can be seen from Fig. 2B that the *MI* values differed from various epochs of seizure, which demonstrated the temporal specificity of PAC along the whole period. Obviously, there existed a strong coupling between the phase of 4-6 Hz oscillations and amplitude of 30-40 Hz oscillations at the mid-seizure epoch.

To further determine the significant difference of *MI* in different co-modulograms, we compared the

MI values of 4-6 Hz and 30-40 Hz oscillations among the five seizure epochs. Box plots of *MI* values of the five epochs were shown in the right panel of Fig. 2B. All *MI* values in the box plot were statistically significant ($p<0.05$, permutation test). As can be seen from the box plot, the *MI* had a significant increase at mid-seizure epoch and a significant decrease at the seizure-termination and post-seizure epochs ($p<0.001$, Kruskal-Wallis test).

The co-modulograms at five seizure epochs and their corresponding box plots in one selected channel of seven patients (12 recorded seizures totally) were illustrated in Fig. 4. As can be seen from the figure that, strong *MI* appeared in the mid-seizure epoch in all 12 recorded seizures of all patients. For patient A, strong phase-amplitude modulation was observed between 4-6 Hz and 30-40 Hz or 30-50 Hz oscillations in three seizures (Seizure 1, Seizure 2 and Seizure 3), which belonged to θ oscillation in LFO and γ oscillation in HFO. For patient B (Seizure 4), strong modulation existed in 6-8 Hz and 60-100 Hz oscillations, i.e., θ oscillation in LFO, γ and ripple oscillations in HFO. Similarly, patient C (Seizure 5) has a strong modulation in 4-5 Hz and 30-80 Hz oscillations, which were in the range of θ oscillation in LFO and γ oscillation in HFO. Unlike patient A, B and C, LFO of patient D (Seizure 6 and Seizure 7) remained in α oscillation modulating the γ and ripple oscillations in HFO. The LFO of patient E (Seizure 8 and Seizure 9) and F (Seizure 10 and Seizure 11) was observed in δ oscillation modulating the γ or ripple oscillation in HFO. For patient G (Seizure 12), γ and ripple oscillations were modulated by the 7-9 Hz oscillations in LFO. The LFOs and HFOs of strong phase-amplitude modulation at mid-seizure epoch of each patient were illustrated in Table 2. The strong phase-amplitude modulating LFOs and HFOs at mid-seizure epoch of 12 seizures (seven patients) were mainly δ、θ、α oscillations and γ、ripple oscillations, respectively. In addition, *MI* values of seizure-specific frequency oscillations at five seizure epochs were made a

comparison of significant difference by box plots (right panel of Fig. 4). All *MI* values in the box plots had statistical significance ($p<0.05$, permutation test). It can be seen from all box plots that the *MI* values at mid-seizure epoch were significantly larger than that at other four seizure epochs (pre-seizure、seizure onset、seizure-termination and post-seizure epochs) ($p<0.001$, Kruskal-Wallis test). These results demonstrate that the modulation between the phase of LFOs and amplitude of HFOs differs during different epochs of temporal seizure. Temporal seizure make the low-frequency phase and high-frequency amplitude have the strong modulation between δ、θ、α oscillations and γ、ripple oscillations in the middle seizure period rather than other seizure epochs and non-seizure period.

[Insert Fig. 4]

[Insert Table 2]

3.2 Spatial specificity of phase-amplitude modulation at mid-seizure epoch.

As can be seen from the co-modulograms at seizure epochs in the selected channel of 12 recorded seizures that, mid-seizure epoch exhibited significantly strong phase-amplitude modulation (Fig. 4). We considered the hypotheses that whether the phase-amplitude modulation at mid-seizure epoch differed in different regions of left and right temporal cortex, and whether the spatial specificity of phase-amplitude modulation related to the location of the epilepsy lesions. Therefore, we computed the co-modulogram at mid-seizure epoch in all channels from 12 seizures of 7 patients. Fig. 5A showed the co-modulograms at mid-seizure epoch of 43 channels of patient A (seizure 2). Bad channel 12 on the electrode strip ② implanted in the right hippocampus had been rejected. The distribution of the co-modulogram in each channel was same as that of the electrodes on the arranged strips in Fig. 1B. Co-modulograms in the left hippocampus, left temporal pole, left temporal base and

right hippocampus, right temporal pole, right temporal base were in the left and right panel of the figure, respectively. *MI* values in the co-modulograms were computed between the phase of low-frequency 0.2-10 Hz with the step of 0.1 Hz and the amplitude of high-frequency 11-200 Hz with the step of 1 Hz.

It can be seen from Fig. 5A that the phase-amplitude modulation was notably different and asymmetrical on the left and right side. In the right temporal pole (electrode strip ④) and right temporal base (electrode strip ⑥), the strong phase-amplitude modulation appeared in the channel 21-23, 37-39 and channel 43. Besides, channel 10 in the right hippocampus (electrode strip ②) also had a strong modulation. The strong phase-amplitude modulations existed in these channels were all between the θ and γ oscillations. By contrast, there was no strong phase-amplitude modulation in the left temporal cortex and hippocampus. Co-modulograms of mid-seizure epoch for all channels of other patients were distinct in different regions of temporal cortex and hippocampus. These results illustrated that the modulation between HFOs and LFOs varied among channels at mid-seizure epoch, which means the spatial specificity of phase-amplitude modulation of temporal lobe epilepsy.

In addition, in order to know whether the PAC modulation strength varies across different electrode channels, we computed the median values of *MI* between seizure-specific LFOs and HFOs at mid-seizure epoch in each seizure of all patients. Fig. 5B showed the median values of *MI* between LFO 4-6 Hz and HFO 30-40 Hz of all 43 channels on both left and right hippocampi and temporal lobes of patient A (seizure 2). This patient underwent the right temporal lobe resection, whose resected channels were marked with light gray rectangle in the figure. As can be seen from Fig. 5B that the high *MI* values existed in channel 10, 21-23, 37-39, 43 (white asterisk *) and the *MI* values of these channels were significantly larger than that of other ipsilateral and contralateral channels

($p<0.001$, Kruskal-Wallis test). The *MI* values of epileptic focus at mid-seizure epoch were also significantly larger than that of other channels in other patients. These results demonstrated the spatial specificity of PAC strength at mid-seizure period. i.e., strong PAC appears in the epileptic focus rather than the normal cortex of temporal lobe epilepsy.

[Insert Fig. 5]

To further evaluate the relationship between the spatial specificity of phase-amplitude modulation at mid-seizure epoch and epilepsy lesion, we compared the channels with strong *MI* in co-modulogram, seizure onset channels identified by the neurosurgeons and the resection channels in the clinical surgery of all 12 recorded seizures. Channels with different features of each patient were marked with various symbols on their corresponding electrode strips, which were illustrated in Fig. 6. Asterisk (*) denoted the strong *MI* channels and different color (green, red and blue) of asterisk denoted different recorded seizures of each patient. Pound sign (#) indicated the seizure onset channels. Channels filled with gray color indicated the clinical resection zones.

As can be seen from the Fig. 6, almost all the channels with strong *MI* appeared on the corresponding left or right temporal cortex of surgical resection and overlapped with the clinical resection zones in all seven patients. It is important to note that the neurosurgeons generally avoid the functional cortex and resect tissue slightly outside of the defined epileptogenic region to minimize the risk of a secondary surgery. These results illustrate that strong *MI* in mid-seizure period can be the biomarker of epileptogenic cortex area and PAC is a potential measure for lateralization and localization of epileptic focus in temporal lobe epilepsy

[Insert Fig. 6]

3.3 Fall-max pattern of phase-amplitude modulation on epileptic foci.

Because the *MI* only quantifies the coupling strength of low-frequency phase and high-frequency amplitude, the pattern of PAC still remains unclear. Therefore, we investigated the PAC pattern by time-varying phase-amplitude modulogram during the whole period from pre-seizure to post-seizure. We analyzed the modulogram between the phase of LFOs and the amplitude of HFOs of ECoG data from all channels for each patient, where the calculated LFOs and HFOs were patient-specific.

Fig. 7 showed the time-varying modulograms between low-frequency 4-6 Hz and high-frequency 30-40 Hz oscillations of patient A. The time and low-frequency phase (from $-\pi$ to $+\pi$ with a step of $\pi/9$) were indicated on the horizontal and vertical axis, respectively. Two vertical solid lines represented the seizure onset time and seizure termination time. As can be seen from Fig. 7, in the modulograms of almost all channels in the right temporal pole (electrode strip ④) and right temporal base (electrode strip ⑥), the high-frequency (30-40 Hz) amplitudes were largest at the low-frequency (4-6 Hz) phase range $[-\pi, 0]$ that corresponded to the falling edges of LFOs during middle period of seizure, which was called "fall-max" pattern. Moreover, this pattern was relatively obvious in the modulograms of channel 21-23 and channel 37-39 in which the co-modulograms had the strong *MI* values (Fig. 5). By contrast, there was no obvious "fall-max" pattern in the left temporal cortex and left hippocampus. In addition, this "fall-max" pattern also appeared in the middle period of seizure of channels with strong *MI* values in co-modulograms in patient C (seizure 5) and patient D (seizure 6, 7) rather than in all twelve studied seizures. These results demonstrated that the "fall-max" pattern was a remarkable phase-amplitude coupling pattern in the epileptic focus during the period of seizures and also a notable feature of neural oscillations in patients with temporal lobe epilepsy.

[Insert Fig. 7]

To further find out what is “fall-max” pattern in the epileptic focus (i.e., how the low-frequency phase and high-frequency amplitude couple in the ECoG signal) and the difference of oscillation features between epileptic cortex and normal cortex, we selected 3-second ECoG data of low-frequency 4-6 Hz and high-frequency 30-40 Hz oscillations in mid-seizure epoch from one channel in the epileptic cortex (channel 38) and the normal cortex (channel 6) of patient A (seizure 2) respectively. The ECoG data (black line), 4-6 Hz oscillation (dark green line) and its corresponding instantaneous phase (light green line), 30-40 Hz oscillation (light red line) and its corresponding instantaneous amplitude (dark red line) were shown in the left panel of Fig. 8A and Fig. 8B. It can be seen from Fig. 8A that the high-frequency amplitudes were largest only at the falling edges of the LFO where the gray arrows pointed, that is, the large high-frequency amplitudes distributed in the low-frequency phase range [-π, 0], which could be seen in the mid-seizure period of time-varying modulograms in Fig. 7. Moreover, the distribution of normalized mean high-frequency amplitudes at the low-frequency phase range [-π, π] of one mid-seizure epoch of “fall-max” pattern was given in the right panel of Fig. 8A. The large mean amplitudes were also distributed on the phase range [-π, 0]. By contrast, in the Fig. 8B, the high-frequency amplitudes were largest at the peaks, the troughs, the rising edges and the falling edges of the LFO, which means the large high-frequency amplitudes distributed evenly in the low-frequency phase range [-π, π]. These results illustrate that, in mid-seizure period, the LFO and HFO of epileptic cortex evolve into a specific coupling pattern, while they present without any synchronous features in the normal cortex.

[Insert Fig. 8]

4. Discussion

Interictal and ictal ECoG recordings are essential to preoperative assessment of localization of the epilepsy focus for the patients with refractory focal seizures. Neurologists sometimes can not completely determine the seizure onset zones clinically by the interictal and ictal ECoG recordings and they are trying to discover a more efficient and reliable biomarker for assessing epileptogenic zones. In this study, we investigated the temporal and spatial coupling difference of low-frequency phase and high-frequency amplitude of ECoG signals collected from 7 patients with temporal lobe epilepsy by using the measure of phase-amplitude coupling, which described the characteristics of neural oscillations during different periods of seizures and made phase-amplitude coupling to be one significant measure for lateralization and localization of the epileptic focus.

To quantify the strength of phase-amplitude coupling during the period from pre-seizure to post-seizure of all patients, we adopted the modulation index to analyze the intensity change of low-frequency phase (0.2-10 Hz with the step of 0.1 Hz) and high-frequency amplitude(11-400 Hz with the step of 1 Hz). Also, we compared the significant difference of modulation index value at five representative seizure epochs (pre-seizure, seizure onset, mid-seizure, seizure termination and post-seizure epoch). The modulation index in co-modulogram at mid-seizure epoch was significantly stronger than that of other seizure epochs in twelve seizures of all patients (Fig. 3 and Fig. 4). In fact, in the interictal period, there was no phase-amplitude synchronization feature between low-frequency and high-frequency oscillations. Gradually, the low-frequency and high-frequency oscillations tended to present a synchronous oscillation mode after seizure onset. When the seizure developed to the middle seizure period, the neural oscillations between low-frequency and high-frequency showed

a specific and regular synchronization feature, which caused the strong phase-amplitude coupling. After that, this particular synchronization oscillation weakened gradually. It is this regular phase-amplitude synchronous mode between low-frequency and high-frequency oscillations in the middle period of seizures that made a high modulation index value than that of other seizure periods. This significantly strong coupling between low-frequency phase and high-frequency amplitude which is appeared in the middle period of the whole seizure is an important characteristic and could be a biomarker during the temporal lobe epilepsy. However, in previous study, Guirgis et al. used the modulation index to compute the phase-amplitude coupling strength at seizure onset, mid-seizure and seizure termination periods and found the modulation in all three seizure periods (Guirgis et al. , 2015b). Also, phase-amplitude modulation was observed in the low-frequency δ and θ rhythms in their study, while the strong phase-amplitude coupling in our study appeared mainly between the low-frequency δ、θ、α oscillations and high-frequency γ、ripple oscillations. Therefore, the low-frequency and high-frequency oscillations modulation frequency bands vary among patients and the strong phase-amplitude coupling did not just appear in the middle period of seizures, which may be related to patients' different conscious states when neurosurgeons record the epileptic seizures or the different types of epilepsy.

In addition, we investigated the spatial distribution of phase-amplitude coupling strength in mid-seizure epoch of all recorded seizures in order to find out the difference across all channels in the left and right hippocampus and temporal cortex. The co-modulograms and modulation index between seizure-specific low and high frequency oscillations of all channels were calculated to assess the spatial distribution of phase-amplitude coupling strength, and also the relationship

between the spatial phase-amplitude modulation and epilepsy lesion location. The spatial modulation and strength of phase-amplitude coupling at mid-seizure epoch showed the difference and asymmetry between low-frequency and high-frequency oscillations of the epileptic cortex and normal cortex (Fig. 5). Obvious phase-amplitude modulation appeared in the specific channels of each patients. Also, channels with strong modulation index overlapped with the seizure onset channels identified by the neurosurgeons and the resection cortex areas in the clinical surgery (Fig. 6). This spatial specificity of phase-amplitude modulation and phase-amplitude coupling strength demonstrate that the epileptic foci cause the strong and specific phase-amplitude coupling compared to the normal cortex. It provides the neurologists important reference signification for the lateralization and localization of the epilepsy lesion of the patients with temporal lobe epilepsy.

To further determine the pattern of phase-amplitude coupling during the whole period from pre-seizure to post-seizure, especially the mid-seizure epoch, time-varying modulogram was used to describe the phase-amplitude coupling pattern of seizure-specific low and high frequency oscillations (Fig. 7). Obvious ‘‘fall-max’’ pattern was observed in three of the seven patients (six of twelve recorded seizures) in the middle period of the seizures. Although this ‘‘fall-max’’ pattern does not appeared in all twelve studied seizures of all patients, we speculate this phase-amplitude pattern may be discovered in other recorded epileptic seizures. Besides, channels with this ‘‘fall-max’’ pattern in modulograms were the ones with the strong *MI* values in co-modulograms. These results illustrate that low-frequency phase modulates the high-frequency amplitude in a particular way in the middle period of seizures, which also varies among different cortical areas. It has no phase-amplitude coupling pattern at the seizure onset time, while the epileptic foci make the low-frequency and

high-frequency oscillations form a pattern of coupling (‘‘fall-max’’ pattern) after several seconds. However, this ‘‘fall-max’’ pattern vanishes before the seizure termination time rather than continue to the end of the seizure. Besides, the ECoG data, low-frequency oscillation and its corresponding instantaneous phase, high-frequency oscillation and its corresponding instantaneous amplitude were elaborated to illustrate the difference of neural oscillations between epileptic cortex and normal cortex (Fig. 8). The specific phase-amplitude synchronization between low-frequency phase and high-frequency amplitude in epileptic cortex led to a strong phase-amplitude coupling and high modulation index value directly, while the irregular phase-amplitude coupling in the normal cortex resulted in the low modulation index value. The ‘‘fall-max’’ phase-amplitude coupling pattern which is not mentioned in previous studies caused by the epileptic foci in the seizure period may be an important biomarker of epileptogenicity. Neurosurgeons can determine the lateralization and localization of the epilepsy lesion by observing the synchronization modes and characteristics between low-frequency and high-frequency oscillations. The neuropathological mechanisms for the appearance and disappearance of “fall-max” pattern during the period from pre-seizure to post-seizure still need to further investigation.

Nevertheless, our study has some limitations. Only twelve recorded seizures of seven patients were studied. More ECoG data segments of recorded spontaneous seizures of more epilepsy patients can provide more sufficient and worthy information for the characteristics of phase-amplitude coupling during the seizure and non-seizure periods. Future work on different gender, different age groups and different time periods of the day will be necessary to be deeply investigated and compared. Epileptic foci located in various cortical areas may have different influences on the pattern of phase-amplitude

coupling during the seizure period. Also, the data length of the ECoG data segment we selected are limited, which only including the data period from the pre-seizure to post-seizure of all the epilepsy patients. Data of interictal period which have longer time interval with that of the seizure period may contain some neurophysiological information about the phase-amplitude modulation of the epileptic foci.

Overall, the phase-amplitude coupling during the whole period from pre-seizure to post-seizure exhibits different features in the patients with temporal lobe epilepsy. Also, the modulation between low-frequency phase and high-frequency amplitude has spatial specificity on different cortical areas. The spatial specificity of phase-amplitude modulation and the newfound “fall-max” phase-amplitude pattern in the middle period of seizure are the important neurophysiological characteristic and biomarker, which may be a good tool for lateralization and localization of the epileptic foci and provide insight to the underlying neural dynamics of the epileptic seizure.

Conflict of Interest Statement

None of the authors have potential conflicts of interest to be disclosed.

Acknowledgments

This work was supported by National High-tech R&D Pro-gram (863 Program) (2015AA020514); Beijing Municipal Science and Technology Project (No.Z121107001012007 and No.Z131107002813039); Beijing Municipal Administration of Hospitals Clinical Medicine Development for special funding support (XM201401).

References

Alvarado-Rojas C, Valderrama M, Witon A, Navarro V, Le Van Quyen M. Probing cortical excitability using cross-frequency coupling in intracranial EEG recordings: a new method for seizure prediction. 2011 Annual International Conference of the IEEE Engineering in Medicine and Biology Society: IEEE; 2011. p. 1632-5.

Crépon B, Navarro V, Hasboun D, Clemenceau S, Martinerie J, Baulac M, et al. Mapping interictal oscillations greater than 200 Hz recorded with intracranial macroelectrodes in human epilepsy. Brain. 2010;133:33-45.

Edakawa K, Yanagisawa T, Kishima H, Fukuma R, Oshino S, Khoo HM, et al. Detection of Epileptic Seizures Using Phase–Amplitude Coupling in Intracranial Electroencephalography. Scientific reports. 2016;6.

Guirgis M, Chinvarun Y, del Campo M, Carlen PL, Bardakjian BL. Defining regions of interest using cross-frequency coupling in extratemporal lobe epilepsy patients. Journal of neural engineering. 2015a;12:026011.

Guirgis M, Chinvarun Y, Del Campo M, Carlen PL, Bardakjian BL. Defining regions of interest using cross-frequency coupling in extratemporal lobe epilepsy patients. J Neural Eng. 2015b;12:026011.

Ibrahim GM, Wong SM, Anderson RA, Singh-Cadieux G, Akiyama T, Ochi A, et al. Dynamic modulation of epileptic high frequency oscillations by the phase of slower cortical rhythms. Exp Neurol. 2014;251:30-8.

Imamura H, Matsumoto R, Inouchi M, Matsuhashi M, Mikuni N, Takahashi R, et al. Ictal wideband ECoG: direct comparison between ictal slow shifts and high frequency oscillations. Clin Neurophysiol. 2011;122:1500-4.

Kanazawa K, Matsumoto R, Imamura H, Matsuhashi M, Kikuchi T, Kunieda T, et al. Intracranially recorded ictal direct current shifts may precede high frequency oscillations in human epilepsy. Clinical Neurophysiology. 2015;126:47-59.

Kerber K, Dümpelmann M, Schelter B, Le Van P, Korinthenberg R, Schulze-Bonhage A, et al. Differentiation of specific ripple patterns helps to identify epileptogenic areas for surgical procedures. Clin Neurophysiol. 2014;125:1339-45.

Mukamel EA, Pirondini E, Babadi B, Wong KF, Pierce ET, Harrell PG, et al. A transition in brain state during propofol-induced unconsciousness. J Neurosci. 2014;34:839-45.

Mukamel EA, Wong KF, Prerau MJ, Brown EN, Purdon PL. Phase-based measures of cross-frequency coupling in brain electrical dynamics under general anesthesia. Conf Proc IEEE Eng Med Biol Soc. 2011;2011:1981-4.

Nonoda Y, Miyakoshi M, Ojeda A, Makeig S, Juhász C, Sood S, et al. Interictal high-frequency oscillations generated by seizure onset and eloquent areas may be differentially coupled with different slow waves. Clin Neurophysiol. 2016;127:2489-99.

Pearce A, Wulsin D, Blanco JA, Krieger A, Litt B, Stacey WC. Temporal changes of neocortical high-frequency oscillations in epilepsy. J Neurophysiol. 2013;110:1167-79.

Ren L, Terada K, Baba K, Usui N, Umeoka S, Usui K, et al. Ictal very low frequency oscillation in human epilepsy patients. Annals of neurology. 2011;69:201-6.

Tort AB, Komorowski R, Eichenbaum H, Kopell N. Measuring phase-amplitude coupling between neuronal oscillations of different frequencies. J Neurophysiol. 2010;104:1195-210.

Figure legends

Fig. 1. (A) Three-dimensional distribution of electrode strips of patient A. The electrode strip ① and ② with purple color were implanted in both left (6×1, channel 1-6) and right (6×1, channel 7-12) hippocampi. The electrode strips ③,④,⑤ and ⑥ with green color were implanted in the left (8×1, channel 13-20) and right (8×1, channel 21-28) temporal pole, also in the left (8×1, channel 29-36) and right (8×1, channel 37-44) temporal base. The blue numbers marked besides the electrode strips denote the channel number on the strips. (B) Planar distribution of all arranged electrode strips of patient A.

Fig. 2. (A) Preprocessed ECoG data of channel 38 from patient A during the period from pre-seizure to post-seizure. Two red dotted line denote the seizure onset time t_{SO} and seizure termination time t_{ST} respectively. The gray rectangles indicates the five selected 10-second seizure epochs, i.e., pre-seizure (I), seizure onset (II), mid-seizure (III), seizure termination (IV) and post-seizure (V). (B) PAC co-modulograms set between the phase of 0.2-10 Hz with the step of 0.1 Hz and the amplitude of 11-200 Hz with the step of 1 Hz of five seizure epochs and corresponding box plot of *MI* values in the co-modulograms between 4-6 Hz and 30-40 Hz oscillations among the five epochs. The notation * indicate significant difference of *MI* values at $p<0.001$.

Fig. 3. Presentation of the phase-amplitude analysis procedures in a structural scheme.

Fig. 4. PAC co-modulograms at five seizure epochs and the corresponding box plots of *MI* values of one selected channel from totally 12 recorded seizures of 7 patients. Frequency for phase (0.2-10 Hz

with the step of 0.1 Hz) and amplitude (11-200 Hz with the step of 1 Hz) were indicated on the horizontal and vertical axis, respectively.

Fig. 5. (A) PAC co-modulograms at mid-seizure epoch from all channels of patient A (Seizure 2). Frequency for phase (0.2-10 Hz with the step of 0.1 Hz) and amplitude (11-200 Hz with the step of 1 Hz) were indicated on the horizontal and vertical axis, respectively. (B) *MI* values between 4-6 Hz and 30-40 Hz at mid-seizure epoch from all channels of patient A (seizure 2). Strong *MI* channels are marked with white asterisk *.

Fig. 6. Channels marked with different symbols which represented strong *MI* channels in co-modulogram (*), seizure onset channels identified by the neurosurgeons (#) and the resection channels in the clinical surgery (gray electrode) of all 12 recorded seizures from 7 patients.

Fig. 7. Time-varying phase-amplitude modulograms during the period from pre-seizure to post-seizure from all channels of patient A (Seizure 2). The seizure onset time (t_{SO}) and seizure termination time (t_{ST}) are demarcated by the black vertical lines in each modulogram.

Fig. 8. The ECoG signals of epileptic cortex (A) and normal cortex (B) at mid-seizure epoch (left panel) and their corresponding distribution of normalized mean amplitudes of high-frequency oscillation at the low-frequency phase range $[-\pi, \pi]$ (right panel).

Tables

Table 1. Clinical characteristics of seven patients.

Patients/ Seizure Number	Sex	Age (years)	Epilepsy duration (years)	Seizure semiology	MRI findings	MEG abnormal current source	Interictal EEG	Pathology	Strip electrode placement/Electrode contacts	Resection side	Follow-up period(months)/Surgical outcome (Engel Class)
A/1,2,3	F	24	6	LoC, Bilateral hand automatism, Automatism of right leg; Convulsions of the limbs	RHS	Mainly in LTL	Left posterior temporal sharp waves	HS+FCD IIIa	LH,LTP,LTB,RH,RTP,RTB/44	R	26/I
B/4	F	46	28	LoC, Bilateral hand automatism	No abnormalities	Mainly in LTL, occasionally in RTL	Bilateral sphenoid spikes	FCD I	LTP,LTB,RTP,RTB /32	L	53/II
C/5	M	22	18	Convulsions of the limbs	LHS	-	Bilateral frontal and sphenoid spikes and sharp waves	HS+FCD I	LH,LTB,LPTB,RH,RTB,RPTB /48	L	55/II
D/6,7	M	33	11	Convulsions of the limbs	LHS	Mainly in LTL, occasionally in RTL		severe HS	LH,LTP,LTB,RH,RTP,RTB /38	L	54/I
E/8,9	F	28	19	LoC, Involuntary movements; Convulsions of the limbs	No abnormalities	RTL	Right frontal and central sharp waves	FCD I	RH,RTP,RTB,RPTL,RFPL/64	R	27/I
F/10,11	F	28	23	LoC, Bilateral hand automatism; Eyes on the turn accompanied by nausea; Convulsions of the limbs	Suspected bilateral HS	-	Bilateral sphenoid spikes	FCD I+Gray matter heterotopia	LTP,LTB,LTO,RTP,RTB,RTO/48	R	34/III
G/12	M	21	18	LoC, Convulsions of the limbs	No abnormalities	-	Bilateral sphenoid sharp waves	HS+FCD IIIa	LTP,LTB,LTO,RTP,RTB,RTO/48	R	29/III

F:female, M:male, L:left, R:right, H: hippocampus, TL: temporal lobe, TP: temporal pole, TB: temporal base, PTL: posterior temporal lobe, PTB: posterior temporal base, FPL: frontal-parietal lobe, TO: temporal-occipital, LoC: loss of consciousness, HS: hippocampal sclerosis, FCD: focal cortical dysplasia

Table 2. Frequency band of oscillation of strong *MI* at mid-seizure epoch of the selected channel in twelve seizures of seven patients.

Seizure/Patient	1/A	2/A	3/A	4/B	5/C	6/D	7/D	8/E	9/E	10/F	11/F	12/G
LFO	θ	θ	θ	θ	θ	α	α	δ	δ	δ	δ	θ & α
HFO	γ	γ	γ	γ & ripple	γ	γ & ripple	γ & ripple	γ	γ	γ & ripple	γ & ripple	γ & ripple

LFO: low frequency oscillation, HFO: high frequency oscillation

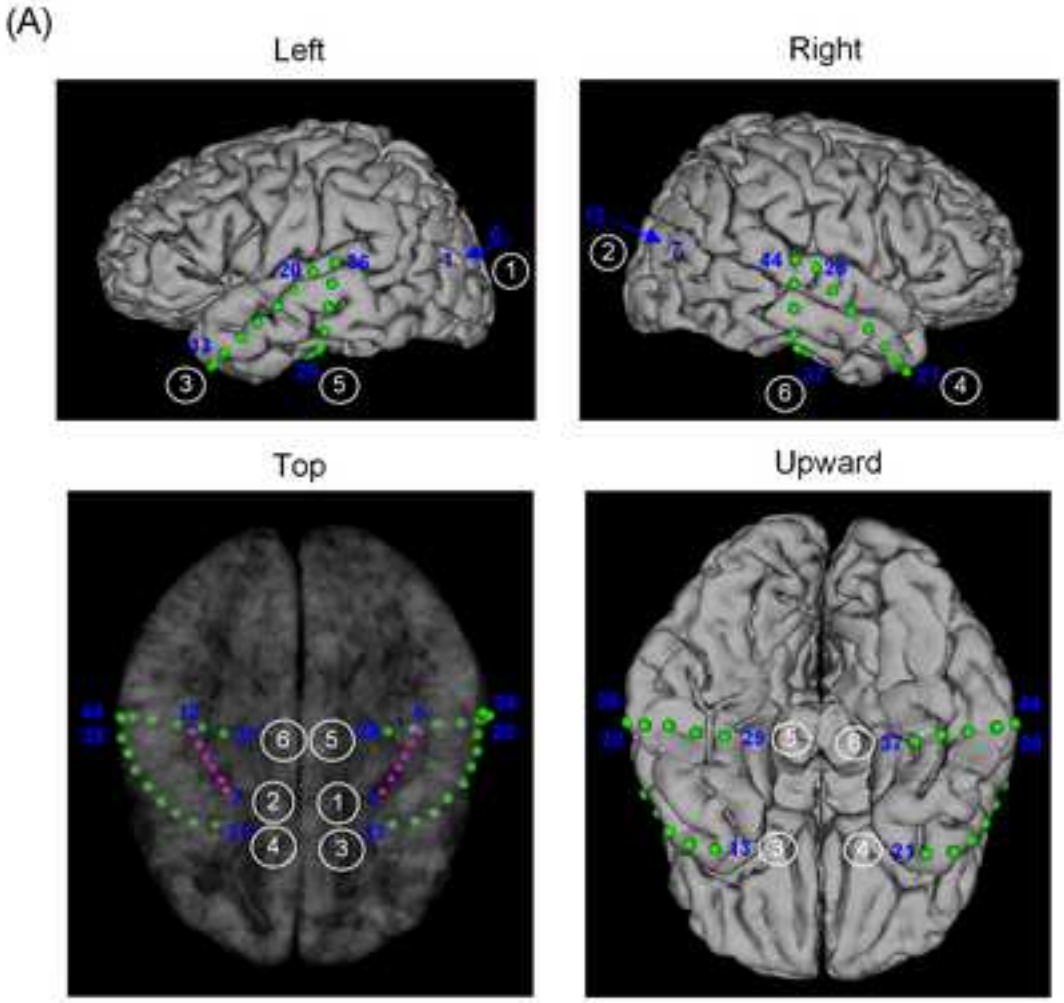

Spatial distribution of electrode strips – Patient A

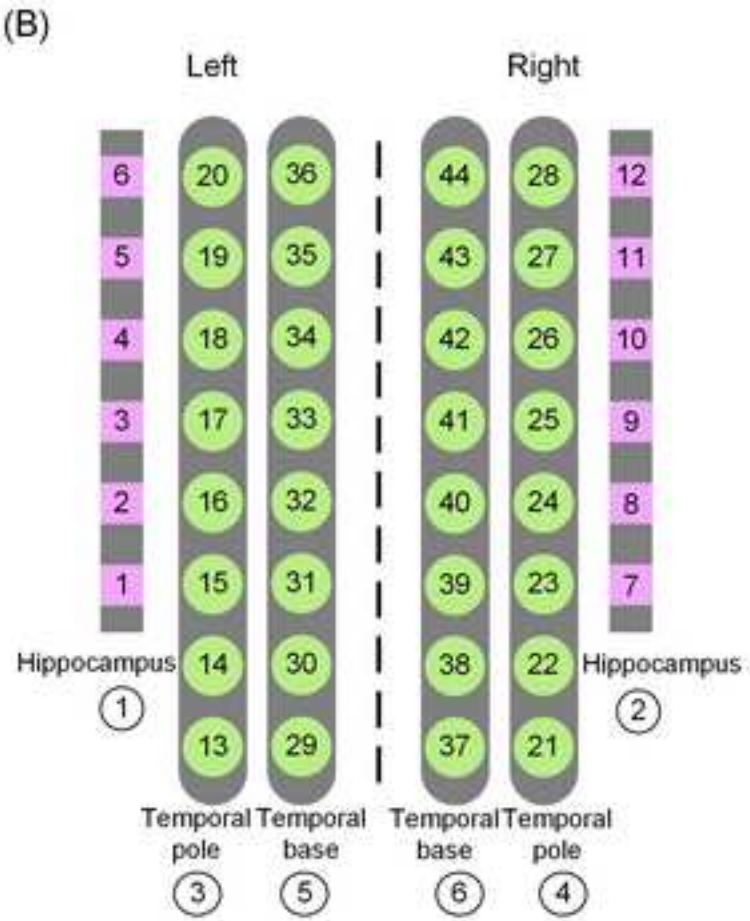

Planar distribution of electrode strips – Patient A

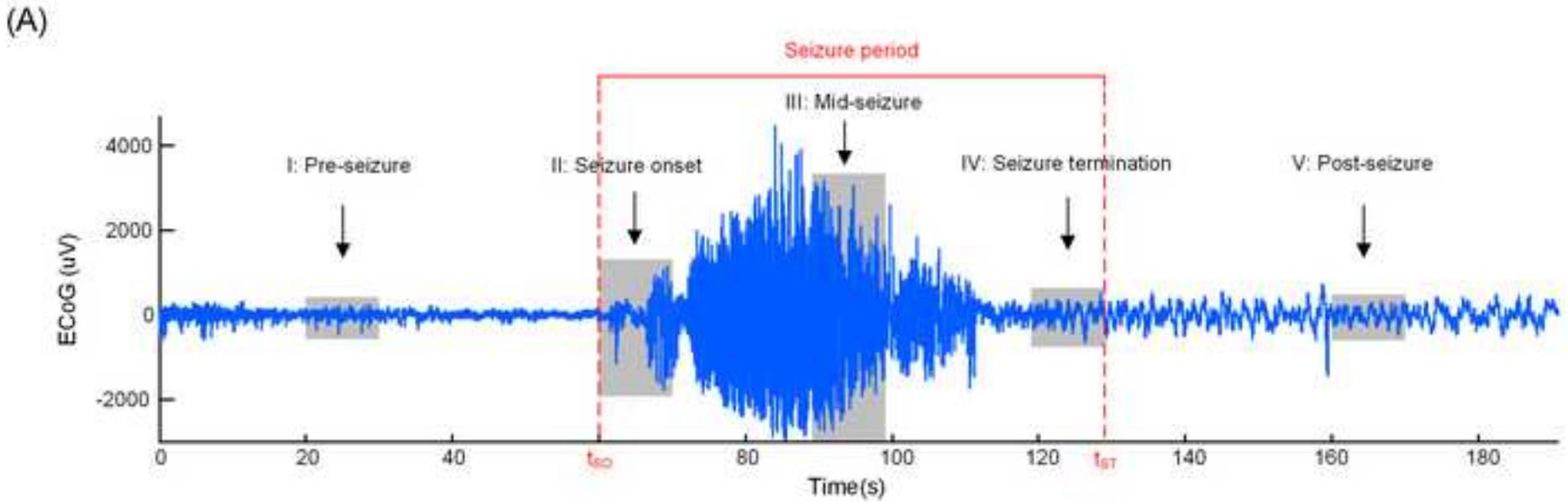

ECoG data of channel 38 – Patient A (Seizure 2)

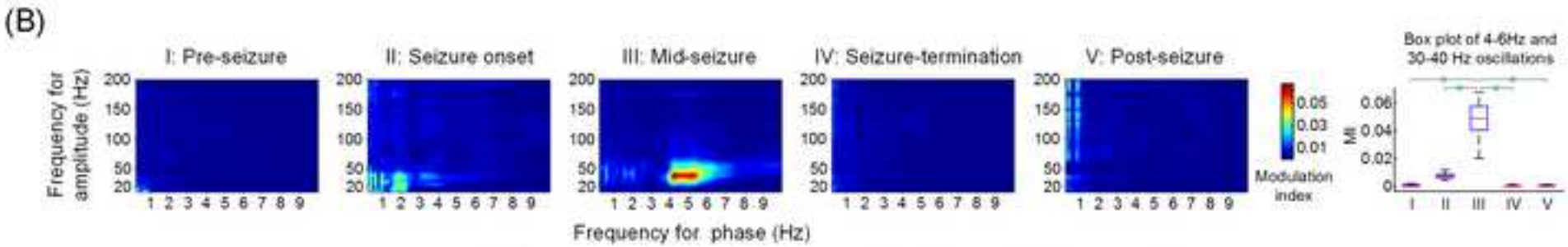

PAC co-modulogram of channel 38 – Patient A (Seizure 2)

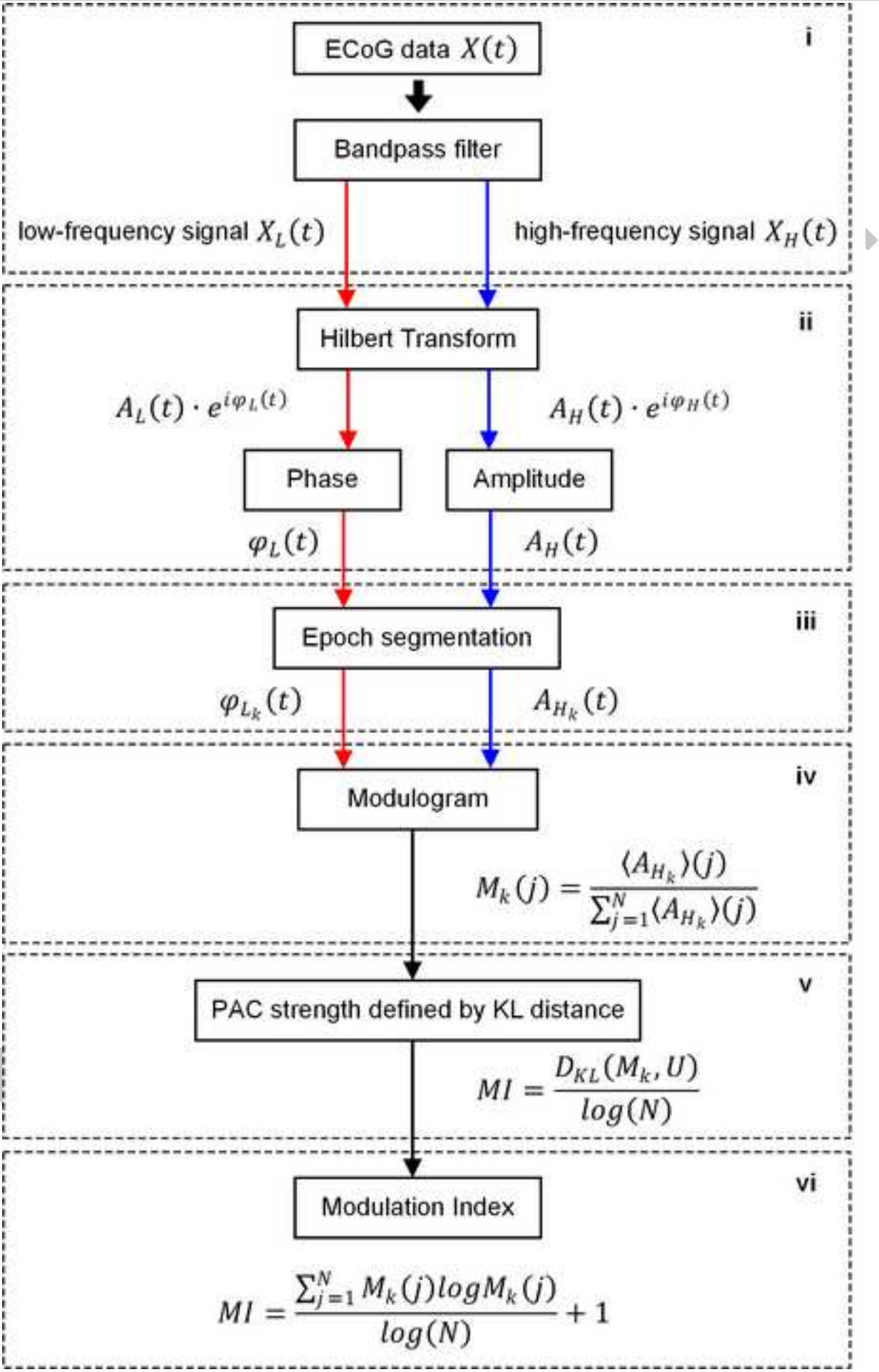

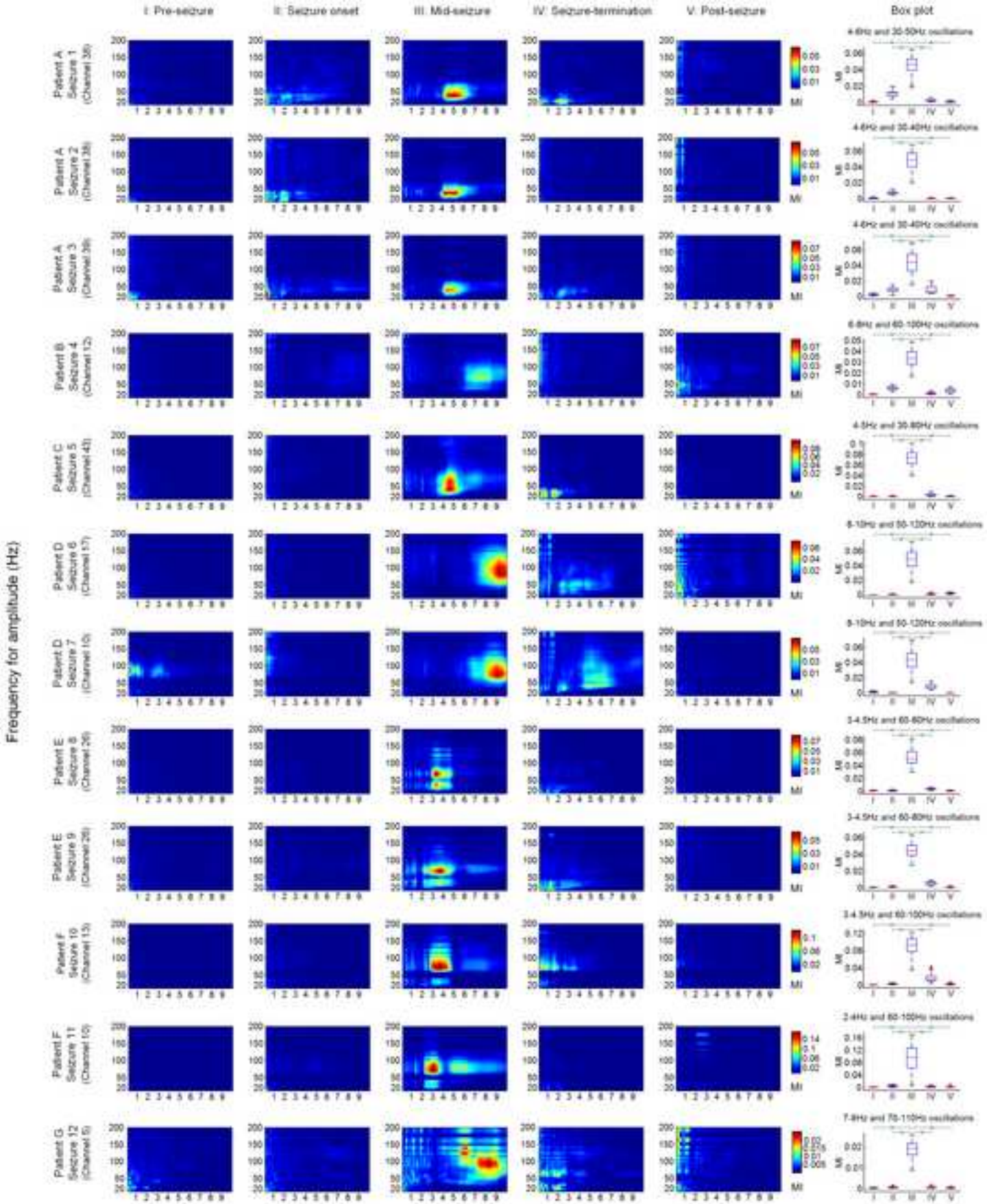

PAC co-modulogram of 12 seizures (7 patients)

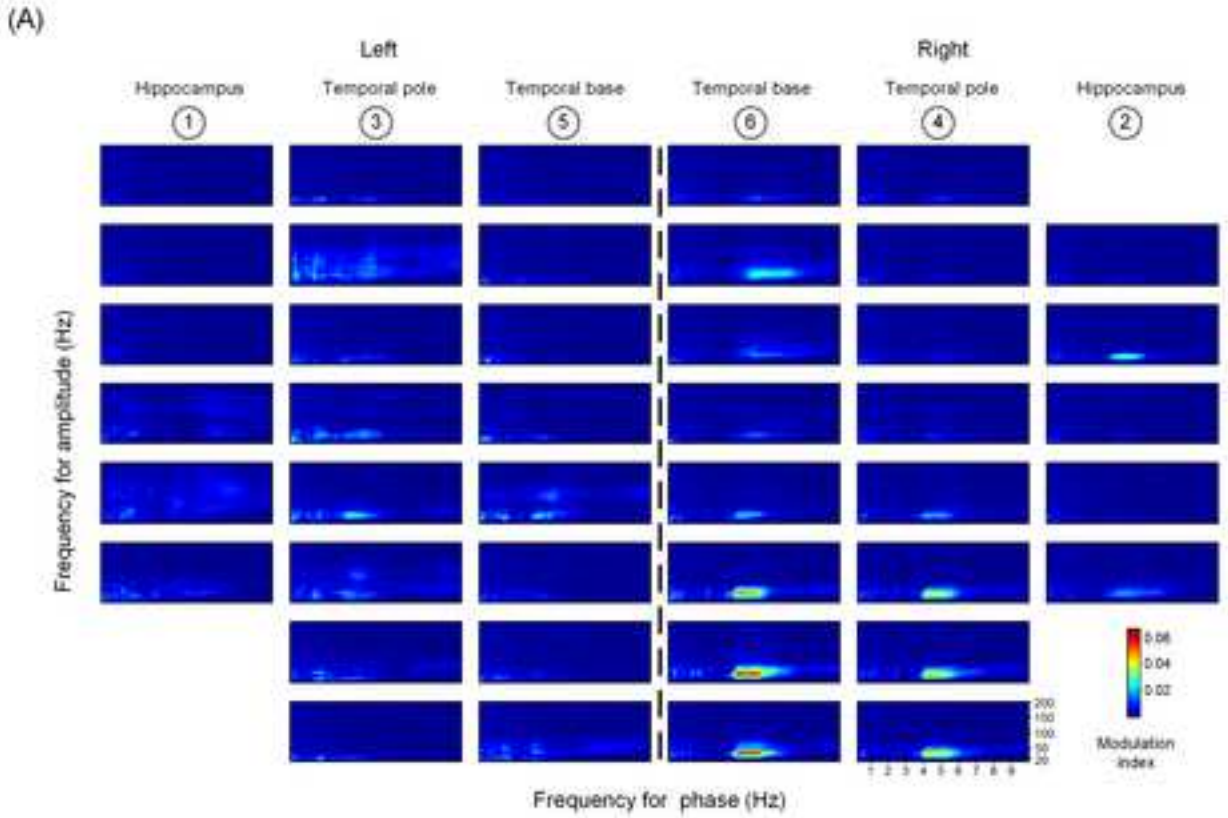

PAC co-modulograms at mid-seizure epoch - Patient A (seizure 2)

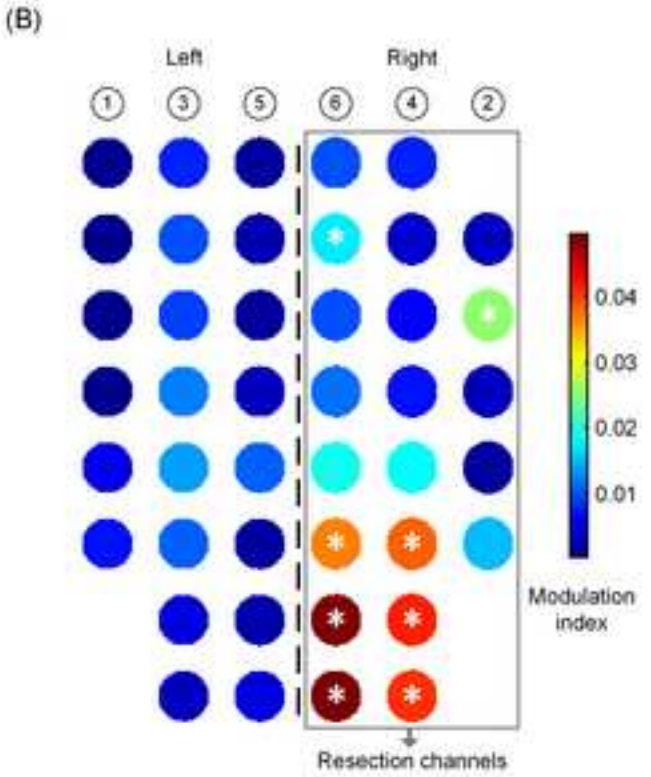

Distribution of MI between 4-6Hz and 30-40Hz oscillations at mid-seizure epoch - Patient A (seizure 2)

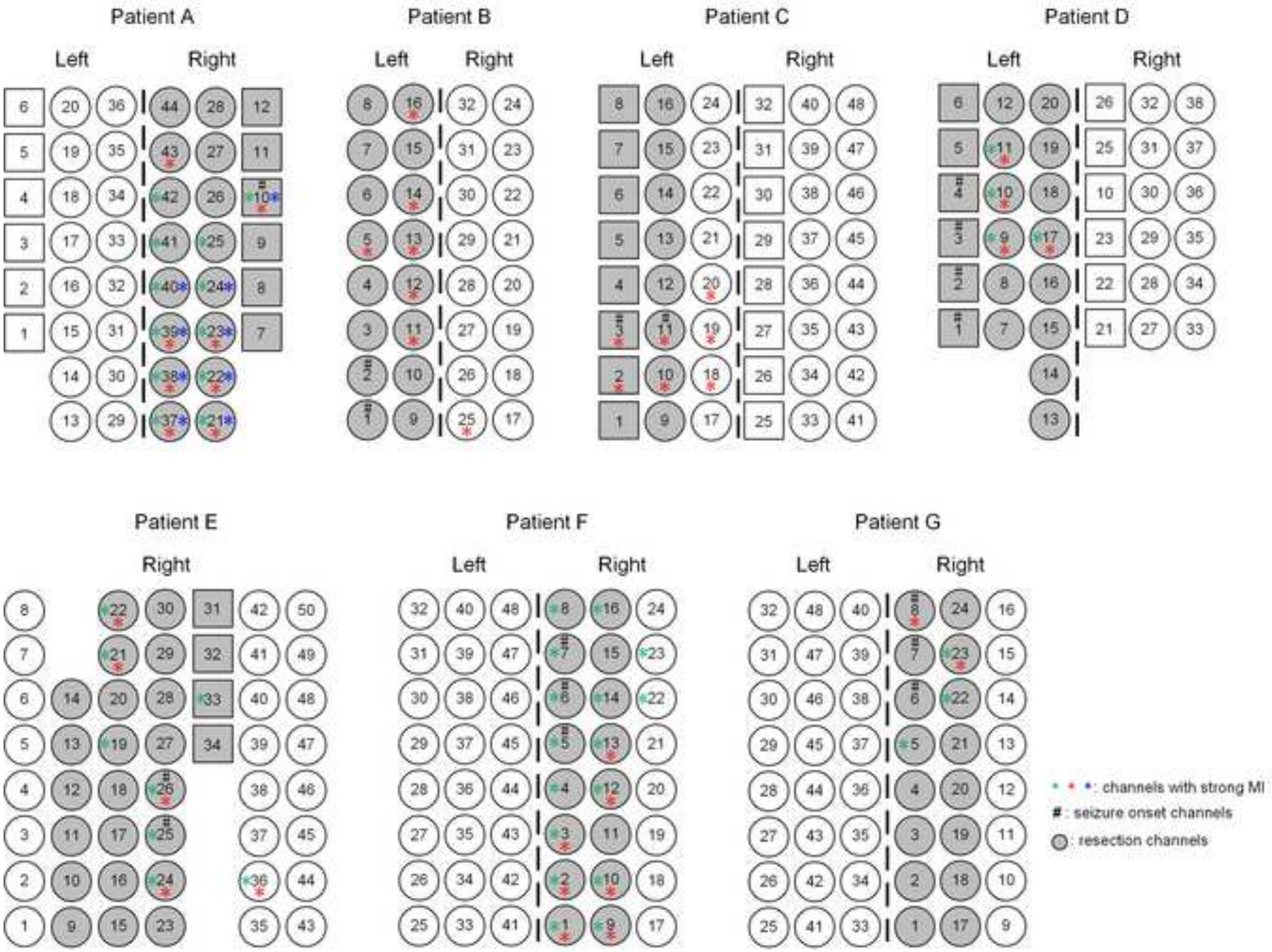

Channels with different features at mid-seizure epoch of all patients

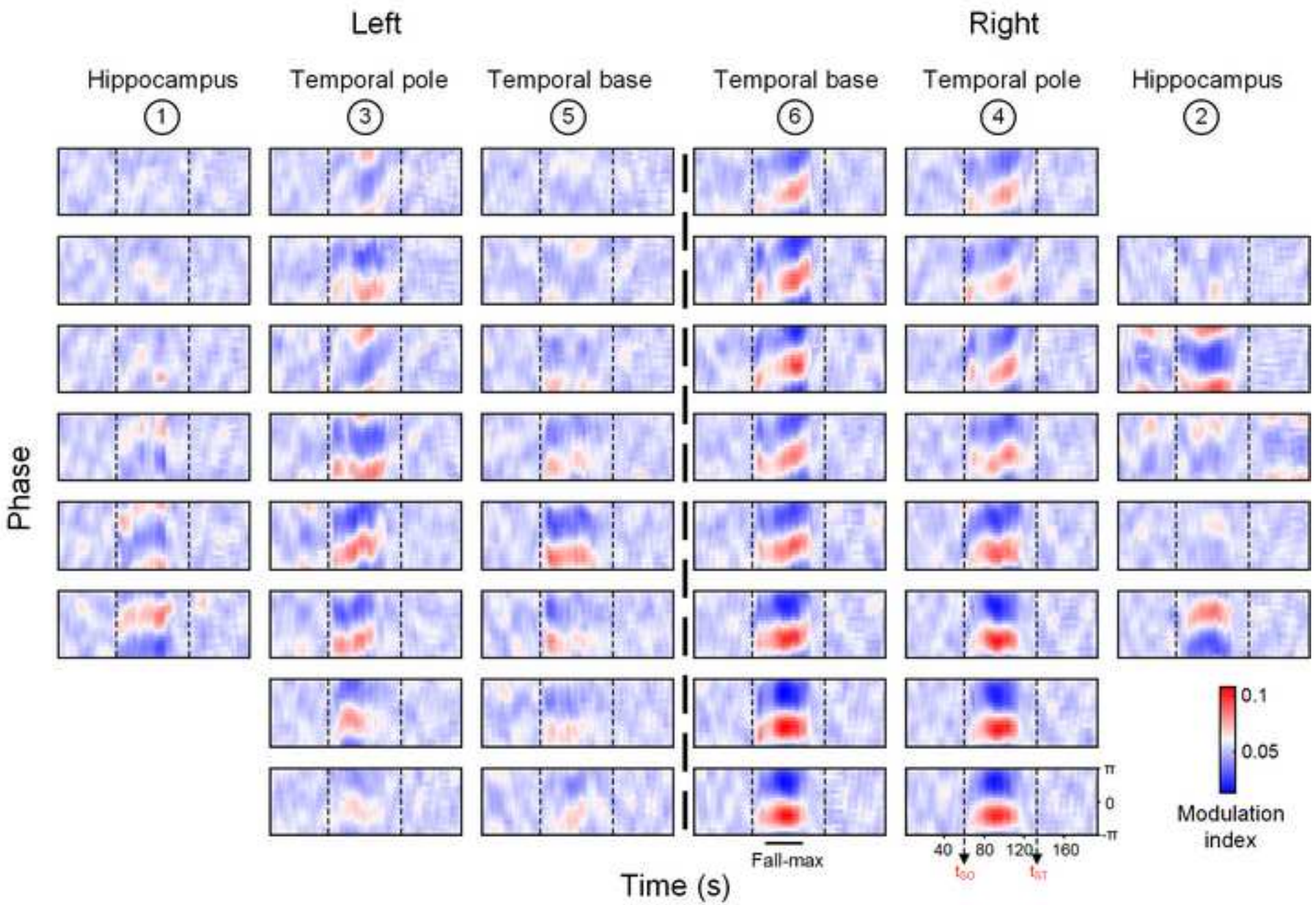

Time-varying modulograms - Patient A (seizure 2)

(A)

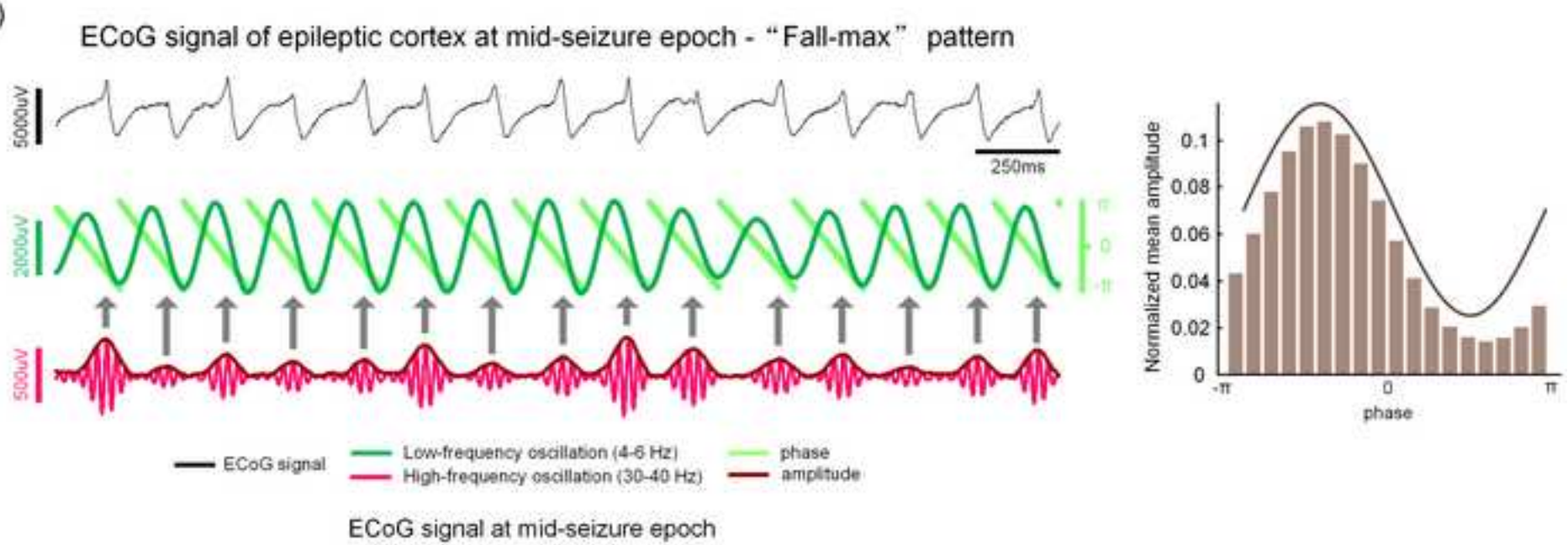

ECoG signal at mid-seizure epoch

(B)